*Curr Oncol*, Vol. 21, pp. e172-178; doi: http://dx.doi.org/10.3747/co.21.1772

LETTER TO THE EDITOR

# Early prediction of treatment response in advanced gliomas with $^{18}$F-DOPA positron-emission tomography

The Editor
*Current Oncology*
August 27, 2013

Imaging markers that enable prediction of survival are of interest for aiding clinical decision-making for patients with advanced glioma. However, current imaging methods based on the use of contrast-enhanced magnetic resonance imaging (MRI) and $^{18}$F-fludeoxyglucose positron-emission tomography (PET) applied in the early stages after treatment are not strongly correlated with patient outcome. In conjunction with MRI, amino-acid PET tracers have shown promise for this application, including variations in L-[methyl-$^{11}$C]-methionine uptake[1] and 3′-dexoy-3′-[$^{18}$F] fluorothymidine (FLT)[2] uptake, and volume variations of regions with high FLT and 6-[$^{18}$F] fluoro-L-DOPA ($^{18}$F-DOPA)[3] uptake.

Uptake of FLT is predictive of survival in recurrent advanced glioma, even when chemotherapy renders MRI unreliable[2]. However, previous serial assessments have typically considered global uptake within the tumour[1,2,4], even though treatment failure frequently occurs locally within areas of existing abnormality[5].

The hypothesis explored here is that poor patient survival is directly related to the extent of the most treatment-resistant cluster of malignant cells exhibiting persistent metabolic activity. Apart from the use of $^{18}$F-DOPA as an early surrogate marker, a key difference between this study and previous work is the longitudinal comparison of metabolic activity within focal peritumoural regions.

The study enrolled 9 patients (7 men; age range: 52–71 years), summarized in Table I, with histopathologically confirmed high-grade brain tumour (World Health Organization grade IV). The institutional ethics review board approved the study, and patients provided informed written consent. Patients received MRI and $^{18}$F-DOPA PET scans at two time points: a baseline immediately before tumour resection, and a follow-up at 12 weeks after resection. The post-resection interval consisted of 2 weeks' recovery, a 6-week course of chemoradiotherapy (external-beam radiotherapy of 60 Gy in 30 fractions or 40 Gy in 15 fractions, with concurrent temozolomide), and 4 weeks' recovery to minimize potential treatment-induced variations in metabolism. (Figure 1 provides a schematic outline.) The PET intensities were normalized to the ipsilateral cerebellum and reported as standardized uptake value ratios. One patient did not receive chemoradiotherapy.

After rigid registration, the most metabolically active voxel in each post-treatment tumour was selected from the PET image. Using nearby anatomic features from the fused MRI, the corresponding location was selected on the pre-surgery image under the guidance of experienced specialists (PT, MF, RLJ, CW, AC) blinded to the pre-treatment PET image and patient outcome. The mean $^{18}$F-DOPA uptake within a 1-cm radius sphere centred on each landmark was calculated before computing the difference between baseline and follow-up. The 1-cm radius traded off the typical statistical variation in PET intensities and potential inaccuracies in spatial correspondences with the size of metabolically active regions. A Cox proportional hazards analysis model was used to evaluate the relationship between variations in $^{18}$F-DOPA uptake and survival.

Survival times, plotted in Figure 2 as a function of change in $^{18}$F-DOPA uptake, ranged from less than 30 weeks to more than 110 weeks. At last report, 3 patients remained alive. Variations in $^{18}$F-DOPA uptake ranged from less than –50% to more than +20%. The results, summarized in Table II, demonstrate that a decrease in $^{18}$F-DOPA uptake is a predictor of extended survival. For interest, the selected regions in each patient are shown in Figures 3–5. A Cox proportional hazards model fitted the data closely ($r = 0.65$), and showed that the hazard to the patient declined by 10.3% with each 1% decrease in local $^{18}$F-DOPA uptake. The null hypothesis—that changes in $^{18}$F-DOPA are not related to survival—was rejected with some significance ($p < 0.032$).

A second model, incorporating age and sex, was compared with the first using analysis of variance

TABLE I Values extracted from each dataset

| *Pt ID* | *Age (years)* | *Sex* | *$^{18}$F-DOPA standardized uptake value ratio*[a] | | | | | | *Survival (weeks)* |
|---|---|---|---|---|---|---|---|---|---|
| | | | *Local* | | | *Global* | | | |
| | | | *Baseline* | *Follow-up* | *Δ (%)* | *Baseline* | *Follow-up* | *Δ (%)* | |
| 01 | 69.5 | Male | 1.93 | 1.81 | –6 | 1.84 | 1.47 | –18 | 45 |
| 02 | 56.8 | Female | 1.73 | 1.48 | –14 | 1.34 | 1.27 | –16 | 56 |
| 03[a] | 71.4 | Male | 1.91 | 0.91 | –52 | 1.28 | 0.89 | –2 | 114 |
| 04 | 62.1 | Male | 1.49 | 1.59 | 7 | 1.19 | 1.28 | –26 | 33 |
| 05[a] | 70.7 | Female | 2.00 | 1.29 | –36 | 1.74 | 1.15 | –8 | 97 |
| 06 | 71.3 | Male | 1.54 | 1.39 | –9 | 1.26 | 1.26 | –11 | 89 |
| 07 | 62.3 | Male | 1.61 | 2.02 | 26 | 1.40 | 1.50 | –38 | 42 |
| 08 | 64.8 | Male | 1.19 | 1.11 | –7 | 1.78 | 1.20 | 5 | 50 |
| 09[a] | 52.6 | Male | 1.24 | 1.24 | –0 | 1.29 | 0.99 | –19 | 42 |

[a] In units normalized to ipsilateral cerebellum.
[b] Patient alive at last report.
Pt = patient.

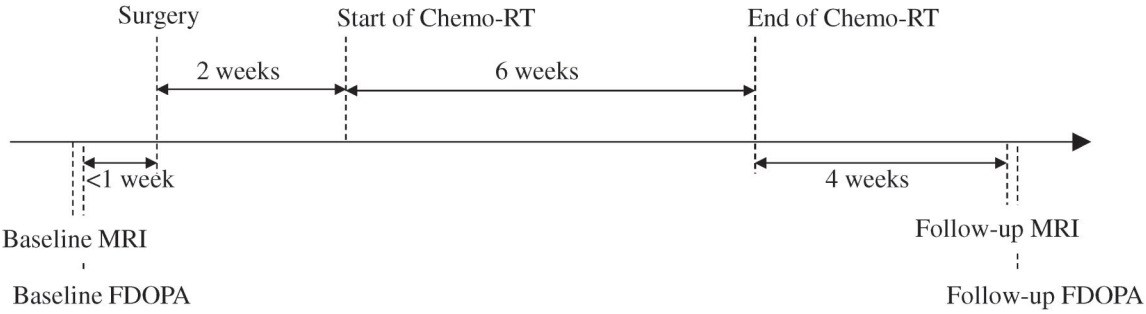


*FIGURE 1 Timing of magnetic resonance imaging (MRI) and $^{18}$F-DOPA positron-emission tomography (FDOPA). Both modalities were used at two time points: once before surgery and once 12 weeks after surgery. Chemo-RT = chemoradiation therapy.*

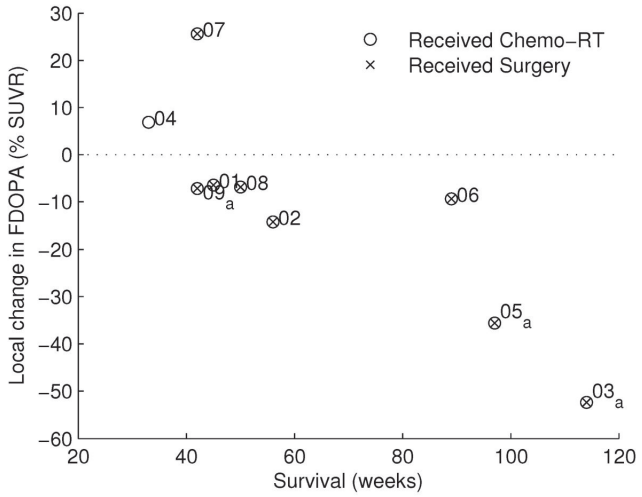


*FIGURE 2 Plot of survival versus local change in the spherical region centred on the point of greatest metabolism after treatment. A value of 0% (dotted line) indicates no change in $^{18}$F-DOPA uptake. Chemo-RT = chemoradiation therapy. [a] Patient was alive at last report.*

TABLE II Statistics extracted from all patients

| *Statistic* | *Local*[a] | *Global*[b] |
|---|---|---|
| Hazard ratio (%/unit Δ) | 10.3 | 5.2 |
| $r^2$ | 0.65 | 0.33 |
| *p* Value (Wald test) | 0.032 | 0.10 |
| *p* Value (likelihood ratio) | 0.002 | 0.056 |

[a] Spherical region of interest.
[b] Entire tumour.

(Table III). The comparison showed that the models largely overlapped ($p > 0.7$), and consecutive increases for log likelihood (4.74 for change in local $^{18}$F-DOPA, 0.24 for age, and 0.23 for sex) indicated that age and sex had a more limited influence on the results. Finally, global $^{18}$F-DOPA uptake (mean over the entire tumour) was compared with survival. Compared with local $^{18}$F-DOPA, global $^{18}$F-DOPA was less correlated with survival (5.2% decline in hazard for 1% decrease in uptake), had a poorer fit ($r = 0.33$), and was less significant ($p < 0.1$).

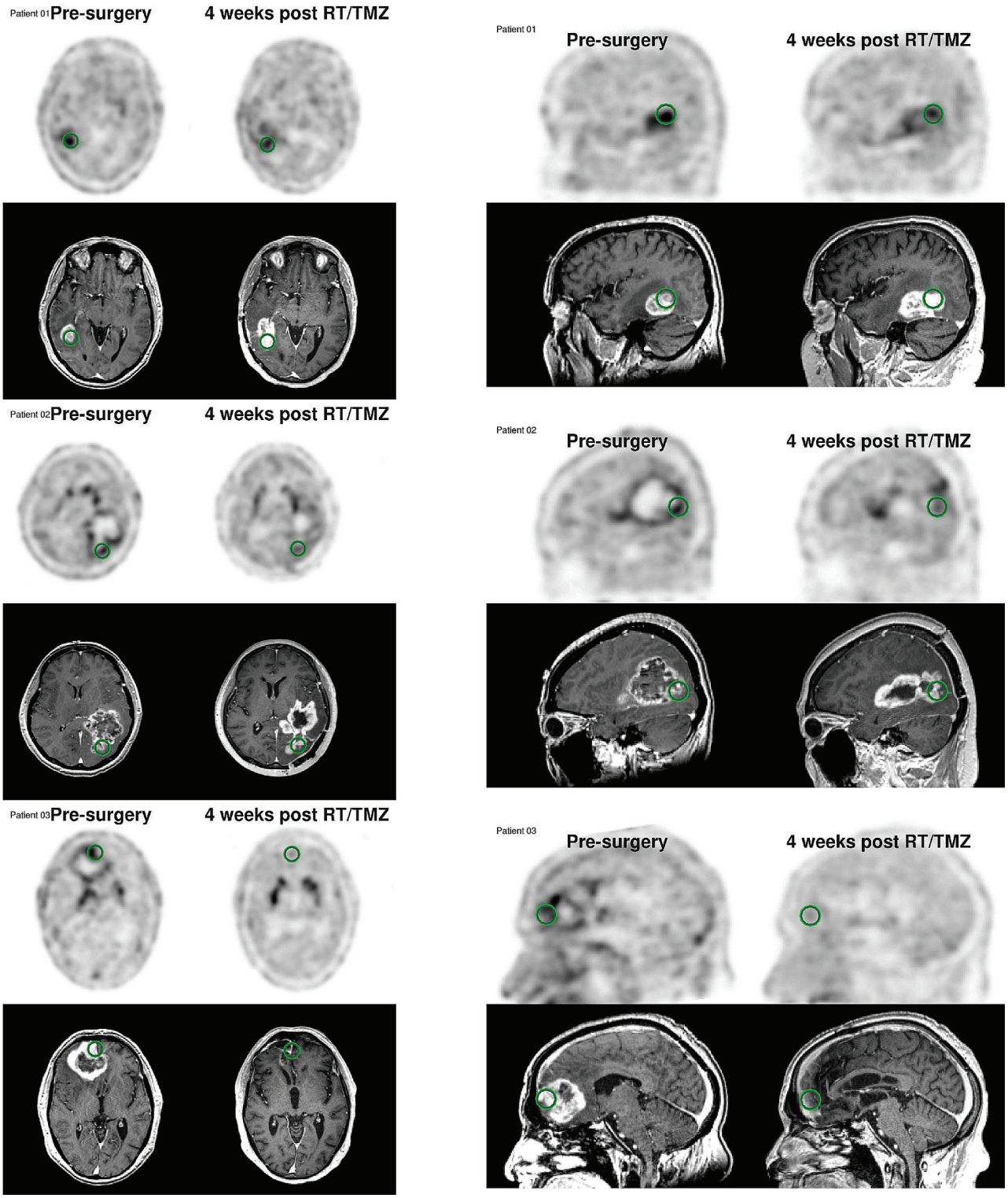


*FIGURE 3 The spherical region of interest (green circles) superimposed on the $^{18}$F-DOPA positron-emission tomography (PET) and contrast-enhanced magnetic resonance imaging (MRI) images for patients 1–3 at baseline and follow-up. Baseline images were acquired before tumour resection (left side of image pairs) and at 4 weeks after chemoradiation therapy (right side if image pairs). In PET images, the standardized uptake value ratio is in the 0–3 range, normalized by ipsilateral cerebellum. The initial point was centred on the highest uptake point in the follow-up PET image and propagated to the follow-up MRI image. While blinded to the PET images and patient outcomes, the reader selected the corresponding point in the baseline MRI image. The selected point was propagated to the fused baseline PET image. RT = radiation therapy; TMZ = temozolomide.*

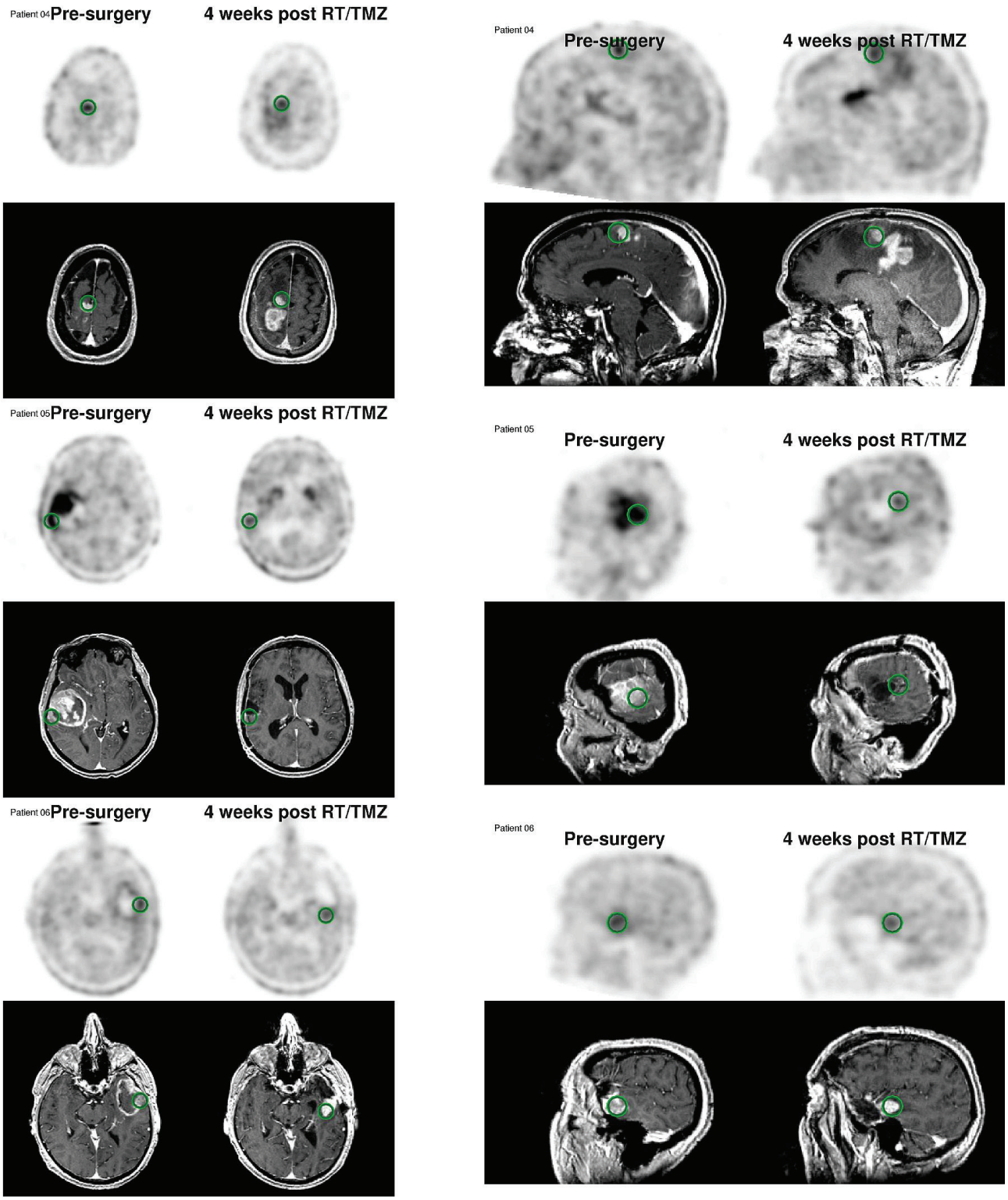


*FIGURE 4 The spherical region of interest (green circles) superimposed on the $^{18}$F-DOPA positron-emission tomography (PET) and contrast-enhanced magnetic resonance (MR) images for patients 4–6 at baseline and follow-up. Baseline images were acquired before tumour resection (left side of image pairs) and at 4 weeks after chemoradiation therapy (right side of image pairs). In PET images, the standardized uptake value ratio is in the 0–3 range, normalized by ipsilateral cerebellum. The initial point was centred on the highest uptake point in the follow-up PET image and propagated to the follow-up MR image. While blinded to the PET images and patient outcomes, the reader selected the corresponding point in the baseline MR image. The selected point was propagated to the fused baseline PET image. RT = radiation therapy; TMZ = temozolomide.*

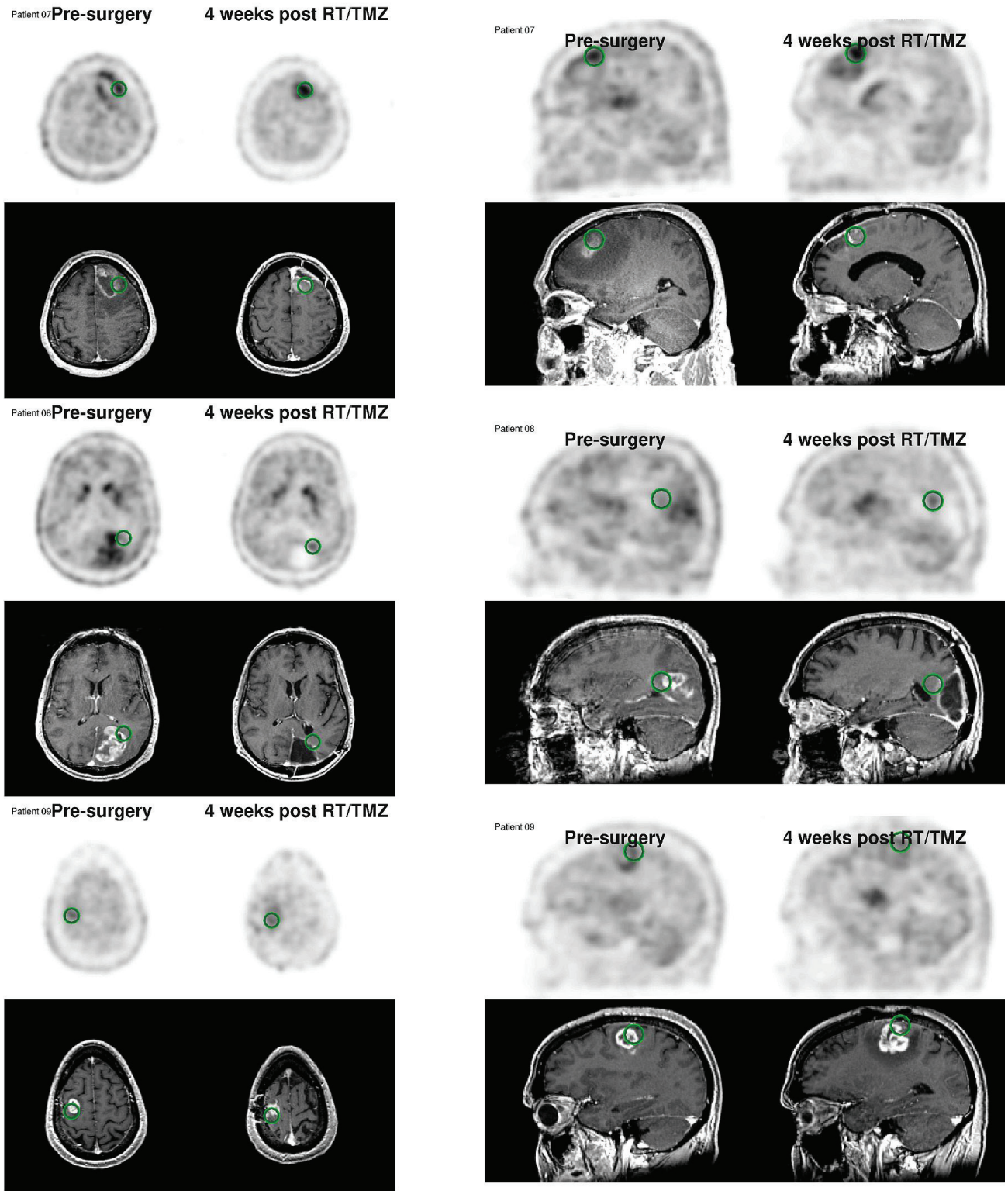


*FIGURE 5 The spherical region of interest (green circles) superimposed on the $^{18}$F-DOPA positron-emission tomography (PET) and contrast-enhanced magnetic resonance (MR) images for patients 7–9 at baseline and follow-up. Baseline images were acquired before tumour resection (left side of image pairs) and at 4 weeks after chemoradiation therapy (right side of image pairs). In PET images, the standardized uptake value ratio is in the 0–3 range, normalized by ipsilateral cerebellum. The initial point was centred on the highest uptake point in the follow-up PET image and propagated to the follow-up MR image. While blinded to the PET images and patient outcomes, the reader selected the corresponding point in the baseline MR image. The selected point was propagated to the fused baseline PET image. RT = radiation therapy; TMZ = temozolomide.*

TABLE III Crude[a] analysis of variance that considers additional effects of age and sex

| *Property* | *Log likelihood of death*[b] | |
|---|---|---|
| | *Cumulative* | *Δ* |
| Baseline[c] | –10.16 | — |
| Δ $^{18}$F-DOPA uptake (% of baseline) | –5.42 | 4.74 |
| Age (years) | –5.18 | 0.24 |
| Sex | –4.95 | 0.23 |

[a] The analysis is considered "crude" because the number of samples is too low for such an analysis. Values in this table should therefore be considered indicative only. Even so, the results indicate that a change in $^{18}$F-DOPA uptake could be more strongly linked with outcome than either sex or age.
[b] Lower is better.
[c] Hazard conferred by membership in cohort.

The more significant correlation between $^{18}$F-DOPA variations locally within tumours (rather than globally), supports the hypothesis that patient survival might be linked to focal points of treatment failure within peritumoural colonies of malignant cells that exhibit enhanced amino-acid uptake after therapy. Hence, variations in $^{18}$F-DOPA are potentially indicative of a genetic predisposition in certain tumours toward treatment sensitivity, with the resulting delay before disease progression leading to extended survival.

These results motivate for the use of $^{18}$F-DOPA–based response criteria as endpoint markers and extend the concept of using $^{18}$F-DOPA–based response criteria to as early as 12 weeks after surgery. Earlier prediction of response could potentially enable early transfer to palliative care if appropriate, early enrolment of patients into therapeutic trials for recurrent tumour, and rapid screening of new therapeutic agents.

Nicholas Dowson PhD
The Australian e-Health Research Centre
Commonwealth Scientific and
Industrial Research Organisation
Royal Brisbane and Women's Hospital
Brisbane, Australia
Nicholas.dowson@csiro.au

Paul Thomas BMed
Specialised PET Services Queensland
Royal Brisbane and Women's Hospital
School of Medicine
The University of Queensland
Brisbane, Australia

Michael Fay MBChB
Department of Radiation Oncology
Royal Brisbane and Women's Hospital
School of Medicine
The University of Queensland
Brisbane, Australia

Rosalind L. Jeffree MBBS MSc
Department of Neurosurgery
Royal Brisbane and Women's Hospital
School of Medicine
The University of Queensland
Brisbane, Australia

Yaniv Gal PhD
School of Information Technology and
Electrical Engineering
The University of Queensland
Brisbane, Australia

Pierrick Bourgeat PhD
The Australian e-Health Research Centre
Commonwealth Scientific and
Industrial Research Organisation
Brisbane, Australia

Jye Smith PhD
Specialised PET Services Queensland
Royal Brisbane and Women's Hospital
Brisbane, Australia

Craig Winter MB BChir
Department of Neurosurgery
Royal Brisbane and Women's Hospital
Brisbane, Australia

Alan Coulthard MBBS BMedSci
Department of Radiology
Royal Brisbane and Women's Hospital
School of Medicine
The University of Queensland
Brisbane, Australia

Olivier Salvado PhD
The Australian e-Health Research Centre
Commonwealth Scientific and
Industrial Research Organisation
Brisbane, Australia

Stuart Crozier BE(Hons) MSc PhD DEng
School of Information Technology and
Electrical Engineering
The University of Queensland
Brisbane, Australia

Stephen Rose PhD
The Australian e-Health Research Centre
Commonwealth Scientific and
Industrial Research Organisation
The University of Queensland
Brisbane, Australia

## CONFLICT OF INTEREST DISCLOSURES

The authors have no financial conflicts of interest to declare.

## REFERENCES


1. Galldiks N, Rapp M, Stoffels G, *et al.* Response assessment of bevacizumab in patients with recurrent malignant glioma using [$^{18}$F]fluoroethyl-L-tyrosine PET in comparison to MRI. *Eur J Nucl Med Mol Imaging* 2013;40:22–33.
2. Chen W, Delaloye S, Silverman DH, *et al.* Predicting treatment response of malignant gliomas to bevacizumab and irinotecan by imaging proliferation with [$^{18}$F] fluorothymidine positron emission tomography: a pilot study. *J Clin Oncol* 2007;25:4714–21.
3. Harris RJ, Cloughesy TF, Pope WB, *et al.* $^{18}$F-FDOPA and $^{18}$F-FLT positron emission tomography parametric response maps predict response in recurrent malignant gliomas treated with bevacizumab. *Neuro Oncol* 2012;14:1079–89.
4. Pafundi DH, Laack NN, Youland RS, *et al.* Biopsy validation of $^{18}$F-DOPA PET and biodistribution in gliomas for neurosurgical planning and radiotherapy target delineation: results of a prospective pilot study. *Neuro Oncol* 2013;15:1058–67.
5. Iwamoto FM, Abrey LE, Beal K, *et al.* Patterns of relapse and prognosis after bevacizumab failure in recurrent glioblastoma. *Neurology* 2009;73:1200–6.